
An adversarial learning algorithm for mitigating gender bias in face recognition

Prithviraj Dhar^{*1}, Joshua Gleason^{*1}, Hossein Souri¹,
Carlos D. Castillo¹, Rama Chellappa¹

¹ University of Maryland, College Park, MD, USA

{prithvi, carlos, rama}@umiacs.umd.edu, {gleason, hsouri}@terpmail.umd.edu

Abstract

State-of-the-art face recognition networks implicitly encode gender information while being trained for identity classification. Gender is often viewed as an important face attribute to recognize humans. But, the expression of gender information in deep facial features appears to contribute to gender bias in face recognition, i.e. we find a significant difference in the recognition accuracy of DCNNs on male and female faces. We hypothesize that reducing implicitly encoded gender information will help reduce this gender bias. Therefore, we present a novel approach called ‘Adversarial Gender De-biasing (AGD)’ to reduce the strength of gender information in face recognition features. We accomplish this by introducing a bias reducing classification loss L_{br} . We show that AGD significantly reduces bias, while achieving reasonable recognition performance. The results of our approach are presented on two state-of-the-art networks.

1 Introduction

Since the introduction of Deep Convolutional Neural Networks (DCNNs), the accuracy of face recognition algorithms has significantly increased [1–5]. The improvement in this technology has led to its usage in a larger number of applications. This has raised concerns about bias against protected categories such as age, gender or race. A recent NIST study [6] found evidence that characteristics such as gender and ethnicity impact the verification and matching performance of existing algorithms. Similarly, [7] showed that most face-based gender classifiers perform better on male faces than female faces. A few works [8–10] have shown that face recognition networks implicitly encode gender information as a by-product of the training process.

Several works [11–18] have recently analyzed and proposed techniques to mitigate bias against race and skintone in face recognition. However, the issue of gender bias in this field has not been widely explored. [19, 20] provide detailed analyses of gender inequality in this area. But, to the best of our knowledge, there does not exist a direct strategy for mitigating gender bias in face recognition. In this paper, we demonstrate the existence of gender bias in representations learned using SOTA face recognition networks, and propose an approach for mitigating this bias. We define gender bias (in Eq. 1) as the difference in the face verification performance on male and female faces. Two potential reasons for the resulting bias are dataset imbalance and the implicit encoding of gender-based cues into the deep features during training.

Dataset imbalance: Gender bias can be mainly attributed to gender imbalance in face recognition training datasets. For example, MS1MV2 dataset [4] is one of the largest face databases available. It consists of 59,563 male and 22,499 female identities. Training a DCNN on such imbalanced datasets leads to differences in the discriminative power of its representations, i.e. features extracted for male faces are more discriminative than those of female faces. This in turn leads to a difference in the

^{*}These authors have contributed equally to this work.

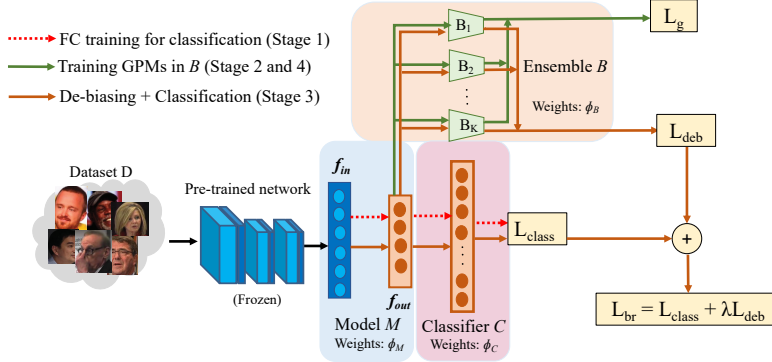


Figure 1: **Adversarial Gender De-biasing (AGD) architecture.** Features f_{in} are extracted from a pre-trained network, and are fed to a model M . M consists of a single linear layer (followed by a PReLU [21] layer) that outputs f_{out} , which is then fed to a classifier C and an ensemble B of gender prediction models (GPMs). The arrows indicate the dataflow at various stages of training. In Stage 1, M and C are trained using L_{class} . In stage 2, GPMs in B are trained using L_g . In stage 3, f_{out} is gender-debiased while being trained to classify identities using L_{br} (applied to M and C). The GPMs are retrained to classify gender using de-biased f_{out} in Stage 4, using L_g . Stage 3 and 4 are run alternatively. More details are included in Sec. 4 and 5.2.

verification performance of male and female faces (i.e. ‘gender bias’). However, as we show in Section 3.2, to obtain similar verification performance on male and female faces, we need to find the appropriate percentage of male and female identities (which may not be 50-50) in the training dataset. Finding such appropriate mixture is not trivial. Therefore, we need an approach that generates fair face representations, irrespective of the gender mix of the training dataset.

Encoding gender information: Recent studies [8, 9] have shown that face recognition networks encode gender information while being trained for identity classification. We believe that encoding of such gender-based cues by face recognition networks also contributes to gender bias. In this work, we mainly focus on this issue and introduce techniques to make face recognition features relatively agnostic to gender. We hypothesize that *reducing the ability to predict gender from face recognition features will reduce the gender bias for verification tasks* (1-1 matching). Therefore, we present an approach called Adversarial Gender De-biasing (AGD), where we introduce a bias reducing classification loss L_{br} , which combines a de-biasing loss (L_{deb}) for adversarially removing gender information from face recognition features, and a classification loss for classifying identities. As a result of reducing gender predictability (either by using a baseline or AGD), we find that gender bias in face verification decreases considerably. To construct the aforementioned baseline, we isolate the components of the feature space which encode gender-specific information using Principal Component Analysis (PCA). Then, we transform the features of test images using the remaining components. Both of these techniques can be used as curative de-biasing measures for pre-trained networks which might be biased as a result of being trained on a gender-imbalanced dataset. Moreover, our proposed techniques do not require any modification to the gender mixture of the training dataset. The conceptual and experimental contributions of our paper are listed below:

- We show that balancing the training dataset to include equal number of male and female identities does not necessarily mitigate the issue of gender bias in face recognition.
- We propose a baseline method - Correlation-based PCA (CorrPCA), to isolate and remove gender-specific components in the feature space using PCA. We transform the face recognition features using the remaining components to perform face verification.
- We propose an approach termed as ‘Adversarial Gender De-biasing’ to unlearn gender information by applying a bias reducing classification loss L_{br} while training face recognition features for classification. This framework (Fig. 1) is trained in a stage-wise manner. The resultant intermediate representations learned in this framework can then be used to perform face verification. We find that AGD significantly outperforms our PCA baseline with respect to bias reduction. Finally, we analyze the bias versus accuracy trade-off for face verification in male and female faces.

2 Related work

Gender bias in deep networks is a critical issue in computer vision. [22] investigates the amplification of gender bias in object classification. This issue is more pressing in face recognition systems. Several empirical studies [6, 7, 18, 19, 23] have shown that current publicly available face recognition

systems demonstrate bias towards attributes such as race and gender. To mitigate bias with respect to a specific attribute, most of the existing methods employ adversarial penalties to make the network agnostic to that attribute, as the network learns to perform the target task. A summary of the such works is given in Table 1. Other than mitigating bias, adversarial de-biasing has also been used for anonymizing representations with respect to chosen attributes. [24] proposes a method to maximally de-correlate the face identity in a given video, while keeping other covariates (such as pose, illumination) unchanged. Wu *et al.* [25] introduce an approach to anonymize identity and private attributes in a given video, while performing the target activity recognition task.

Table 1: Related work summary

Method	Target task	Sensitive attribute
[26, 27]	Analogy completion	Gender
[22]	Object classification	Gender
[25]	Action classification	Identity, private attributes
[28]	Gender/Age prediction	Age/Gender
[29]	Smile, high-cheekbones	Gender, make-up
[30]	Action recognition	Scene
[12]	Face detection	Skintone
[31]	Face attractiveness	Gender
[11]	Face recognition	Race
AGD (Ours)	Face recognition	Gender

Faces, which consist of millions of unconstrained images. Also, in some of the aforementioned experiments, the attribute under consideration is ephemeral to the target task. For example, in [25], an action is not specific to an identity. Similarly, the attractiveness score (computed in [32] and [31]) is not specific to a single gender. Also, presence of smile in [29] may not be unique to a single gender. In contrast, attributes like gender and race may not be ephemeral to face recognition. A given identity can be generally tied to a single gender or race. Therefore, because of the high level of entanglement between identity and gender or race, we believe that disentangling them is more involved. Moreover, it has been already shown in [8, 9] that gender-based cues are important for recognizing identities of facial images. Inspired by existing adversarial de-biasing methods, we propose a framework to reduce the gender information in face recognition features, while making them efficient for the task of identity classification. This approach does not require any modifications to the gender-mix of the training dataset, and can be used for any face descriptor (irrespective of its network).

3 Background

3.1 Gender bias in face recognition

We define gender bias, at a given false positive rate (FPR) as the absolute value of the difference between the verification performance for male-male and female-female pairs.

$$\text{Bias}^{(F)} = |\text{TPR}_m^{(F)} - \text{TPR}_f^{(F)}| \quad (1)$$

where $\text{TPR}_m^{(F)}$, $\text{TPR}_f^{(F)}$ denote the true positive rate for verification of male-male and female-female pairs respectively at a given FPR F . We separately evaluate the face descriptors, obtained using the final fully connected layer of two pre-trained networks:

Network A : Resnet-101 trained on MS1MV2² with Additive Angular margin (Arcface) loss [4]. There are 59,563 males and 22,499 females in this dataset.

Network B : Resnet-101 trained on a mixture of UMDFaces³[34], UMDFaces-Videos³[35] and MS-Celeb-1M [36], with crystal loss [3]. There are 39,712 males and 18,308 females in this dataset. For evaluation, we use the IJB-C dataset, and follow the 1:1 face verification protocol defined in [37]. However, instead of verifying all the pairs, we only verify male-male and female-female pairs separately. There are 6.4 million male-male and 2.1 million female-female pairs defined in the protocol. The gender labels are provided in the dataset. Using networks A and B, we extract 512 dimensional features for aligned facial images in the IJB-C dataset, following which we perform verification of male-male and female-female pairs separately. From Fig 2a, we find that the verification performance for male-male pairs is superior to that for female-female pairs in both networks A and B. This gender bias in face verification is even more apparent at low FPRs (10^{-4} , 10^{-5} , 10^{-6}). The most obvious cause of the gender bias in verification performance of these networks is the gender imbalance in training dataset. We explore this issue in the next subsection.

3.2 Balancing does not help

To investigate the effect of gender mix in the training datasets, we built several alternative datasets, each having a different gender mix. These datasets are built as subsets of a larger combined dataset

²<https://github.com/deepinsight/insightface/wiki/Dataset-Zoo>

³<http://umdfaces.io/>

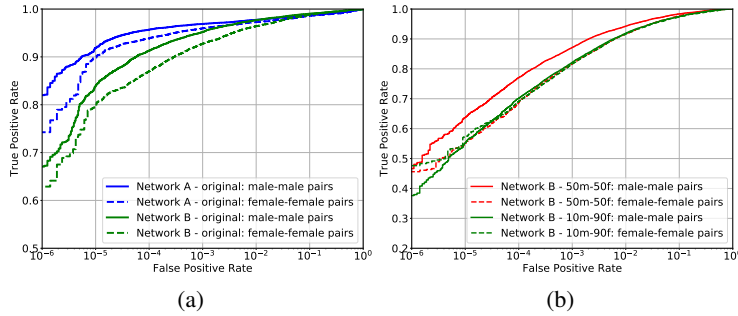


Figure 2: Gender-wise IJB-C face verification results for (a.) original Network A and Network B (b.) Network B trained on datasets with male-female ratio of 1:1 (*50m-50f* dataset) and 1:9 (*10m-90f* dataset) respectively.

of MS-Celeb-1M [36], UMDFaces [34] and UMDFaces-Videos [35]. We fix the number of images $N = 50$ for each identity to be used for training. Subsequently, we select identities having more than $N = 50$ images in the combined dataset. From the selected identities we find that there exist 26,794 male and 14,815 female identities which have greater than $N = 50$ images. We randomly select 14,815 male identities out of the selected 26,794 male identities. Let γ be the percentage of males to be included in the intended dataset. We randomly select $\gamma\%$ of the 14,815 male identities and $100 - \gamma\%$ of the 14,815 female identities to construct the dataset D^γ . Thus, for any given γ , the dataset D^γ always consists of 14,815 identities. Finally, for every identity in D^γ , we randomly select N images to build the final dataset D_N^γ . Fixing $N = 50$, we vary γ from 0 to 100, with an increment size of 10, to construct 11 alternative datasets. Here, D_{50}^{50} (termed as *50m-50f*) is a completely balanced dataset (50% male and female identities), with 50 images for each identity. Using the *50m-50f* dataset, we train a network with the same architecture and loss function as that of Network B. Using the final fully connected layer of this trained network, we extract the features for aligned IJB-C [37] face images (as done in Sec. 3.1), and use them to perform gender-wise face verification. The results of this experiment are presented in Figure 2b. We find that *even after balancing the dataset in terms of gender, the gender-bias issue has not been mitigated.* [20] draws a similar conclusion. We believe that even if the training dataset has equal number of male and female identities, we cannot control the appearance variation in both genders. The difference in the appearance variation in males and females causes the network to demonstrate bias, even if the training dataset is gender-balanced. In our case, we find that using dataset D_{50}^{10} , which has 10% male and 90% female identities (termed as *10m-90f*), balances the recognition capability of the network (see Fig. 2b) on IJB-C. Finding such an appropriate subset of a large dataset is not trivial and will vary for different datasets, which is why balancing the dataset in terms of gender is not scalable. We provide the gender-wise verification results obtained by networks trained on other alternative training datasets (with different gender-mix) in the supplementary material (Section A).

4 Proposed approach

Since balancing the dataset does not necessarily mitigate the issue of gender bias, we target the second reason for existence of bias, described in Section 1, i.e. we obstruct the network features from picking up gender-based cues for classifying identities. In Adversarial Gender De-biasing (AGD), we present a stage-wise approach to learn a model M , which takes features f_{in} as input, and generates their gender-debiased representations f_{out} . f_{out} is fed to an identity classifier C , and to an ensemble B of gender prediction models (GPMs). This approach is presented in Fig. 1. Here, f_{in} is obtained from a pre-trained face recognition network. The loss function for AGD is defined below:

$$L_{br}(\phi_C, \phi_M, \phi_B) = L_{class}(\phi_C, \phi_M) + \lambda L_{deb}(\phi_M, \phi_B) \quad (2)$$

Here, L_{class} is a standard cross-entropy loss for identity classification. ϕ_C, ϕ_M denote the weights of the classifier C and model M in Fig. 1, respectively. L_{deb} is a debiasing loss which is computed using the ensemble of GPMs. We explain this loss in the next subsection. In Eq. 2, λ is used to weight the de-biasing loss, and ϕ_B denotes the weights of all the GPMs in B .

4.1 De-biasing loss L_{deb}

We first extract features f_{in} using a frozen pre-trained network. These features are then fed to a model M consisting of a linear layer (followed by PReLU [21]), to obtain a representation f_{out} .

$$f_{out} = M(f_{in}, \phi_M) \quad (3)$$

We intend to minimize the gender predictability of f_{out} , while also making it proficient for classification. We feed f_{out} to a classification layer, and optimize M and C using L_{class} . Then, using f_{out} as input, we train an ensemble B of K gender prediction models (GPMs), denoted as B_1, B_2, \dots, B_K , to classify gender. Each of these models is a simple MLP network with an input layer of 256 units, a hidden layer with 128 units, a SELU activation layer [38], an output layer of 2 units, followed by a sigmoid and softmax activation layer. The outputs for the i^{th} model in the ensemble, B_i is denoted as:

$$o_i^{male}, o_i^{female} = B_i(f_{out}, \phi_{B_i}) \quad (4)$$

The outputs represent the gender probability scores and ϕ_{B_i} denotes the weights of B_i in the ensemble. After that, for minimizing gender predictability, we feed f_{out} to these trained models and use them as adversaries to model M . Ideally, we would want the model M to produce features with no gender information, so as to confuse the gender prediction models, which would make B_i predict 0.5 as the probability score for both the genders. Hence we compute the adversarial loss for model M , with respect to B_i as follows:

$$L_a^{(B_i)}(\phi_M, \phi_{B_i}) = -(0.5 * \log(o_i^{male}) + 0.5 * \log(o_i^{female})) \quad (5)$$

Here, we use an ensemble of GPMs instead of a single GPM because we want f_{out} to be gender agnostic with respect to multiple gender predictors. This idea has been introduced in [25] to solve ‘the \forall challenge’. After computing the adversarial loss for model M with respect to all the GPMs, we select the one for which the loss is maximum. We term this loss as debiasing loss, L_{deb} .

$$L_{deb}(\phi_M, \phi_B) = \max\{L_a^{(B_i)}(\phi_M, \phi_{B_i})\}_{i=1}^{i=K} \quad (6)$$

The basic idea is that we would like to penalize M , with respect to the strongest GPM, which it was not able to fool. We follow this approach which was introduced in [25]. When L_{deb} is applied to M , ϕ_B remains locked. As defined in Eq. 2, L_{deb} is used in combination with L_{class} , which depends on ϕ_M and ϕ_C . Therefore, the gradient updates for L_{deb} are propagated to ϕ_M and those for L_{class} are propagated to both ϕ_M and ϕ_C .

5 Experiments

In our experiments we evaluate the effectiveness of our proposed approach with respect to gender bias and recognition performance. The experiments were performed on Networks A and B, introduced in Sec. 3.1. These networks achieve SOTA performance on several verification and identification benchmarks. For training, we use a combination of MS-Celeb-1M [36], UMDFaces [34] and UMDFaces-Videos [35] datasets (same as that used to train Network B), which consists of 58,020 identities. We obtain the gender labels for these identities using [39]. For testing, we use the IJB-C [37] dataset, which is an unconstrained face database of 3,531 gender-labeled identities. The IJB-C verification protocol consists of millions of male-male and female-female pairs and the aforementioned networks demonstrate measurable gender bias in this dataset (explained in Sec. 3.1).

5.1 Baseline: CorrPCA

Since our hypothesis (in Sec. 1) involves removing gender specific information from the recognition features, we propose a naive approach, termed as ‘Correlation-based PCA’ (CorrPCA) for this task. We first compute the eigenspace of the features and isolate the eigenvectors which encode gender information. After this, we remove these eigenvectors and transform the test features using the remaining subspace. A similar approach was used in the early nineties [40] to reduce the impact of illumination on PCA features.

Isolating gender specific components: We first randomly select 80k (40k males and females) aligned face images from MS-Celeb-1M dataset. Then, as done in Sec. 3.1, we extract the 512-dimensional feature vector for these images, using a given pre-trained network (Network A or B). We then compute the eigenspace $S \in \mathbb{R}^{512 \times 512}$ of the features $X \in \mathbb{R}^{80k \times 512}$ using PCA. Using each eigenvector in S , we transform the original feature set X as follows :

$$v_s = X \cdot s \quad (7)$$

Here, s is a row (i.e. an eigenvector) in S , and v_s is the transformed output. Now, for all the 80k images, we have a vector $v_s \in \mathbb{R}^{80k \times 1}$ and a label vector ℓ , with gender labels for all the sampled images. After this, we compute the Spearman correlation coefficient between v_s and ℓ . We select the eigenvectors in S for which this correlation is greater than δ and denote them collectively as a set G . Thus, G is a subspace which has relatively higher gender information.

Transforming test features using remaining components: We then extract the 512-dimensional features for IJB-C dataset using the given pre-trained network (Network A or B), to obtain feature set

X_{ijbc} . Finally we transform X_{ijbc} using the eigen-subspace spanned by $S - G$ into a new feature space T_{ijbc} . We use $\delta = 0.1$ in this protocol, for both networks. The detailed algorithm is provided in the supplementary material (Sec. B). The results of this baseline are presented in Sec. 6.1.

5.2 Experimental protocol for AGD

We now explain the various stages of training AGD. We use the notations from Section 4. For training, we use a combination of UMDFaces, UMDFaces-Videos and MS-Celeb-1M dataset. We perform our experiments using input features f_{in} from Networks A and B, extracted for these datasets.

Stage 1 - Fully Connected (FC) Training: Using input features f_{in} from a pre-trained network, we train a fully connected network model M with a 256 dimensional single hidden layer (followed by PReLU activation), and a classifier C . A standard cross-entropy classification loss $L_{class}(\phi_M, \phi_C)$ is used to train M and C for T_{fc} iterations.

Stage 2 - Initializing and training GPMs: Once M is trained to perform classification, we feed the outputs f_{out} of M to an ensemble B of K GPMs: B_1, B_2, \dots, B_K . Each of these GPMs is a simple MLP network, for which the architecture is defined in Section 4.1. This ensemble is trained to classify gender for T_{gtrain} iterations. The GPMs are trained using $L_g(\phi_M, \phi_B)$, which is computed as a sum of the cross-entropy losses of individual GPMs ($L_g^{(B_k)}$) in B :

$$L_g^{(B_k)}(\phi_M, \phi_{B_k}) = -y_i \log y_i^{(k)} - (1 - y_i) \log (1 - y_i^{(k)}) \text{ and } L_g(\phi_M, \phi_B) = \sum_{k=1}^K L_g^{(B_k)} \quad (8)$$

Here, y_i is the binary gender label for i^{th} input feature, and $y_i^{(k)}$ represents the respective softmaxed outputs of B_k in the ensemble. L_g is applied only on the GPMs, and ϕ_M, ϕ_C remain unchanged.

Stage 3 - Classification and de-biasing: Here, M is trained to generate features f_{out} which are proficient in classifying identities and are relatively gender-agnostic. f_{out} is provided to the ensemble B and the classifier C , the outputs of which result in L_{deb} (Eq. 6) and L_{class} respectively. We combine them to compute L_{br} (Eq. 2) for training M and C for T_{deb} iterations, while ϕ_B is locked.

Stage 4 - Re-training GPMs: In stage 3, M is trained to generate gender-debiased features to fool the GPMs in the ensemble, whereas in stage 4 GPMs are re-trained to classify gender using the de-biased features f_{out} from M . Therefore, we run stages 3 and 4 alternatively, for E episodes, after which we re-initialize and re-train all the GPMs (as done in stage 2). Here, one episode indicates an instance of running stage 3 and 4 consecutively. In stage 4, we heuristically choose one of the GPMs in the ensemble, and train it until it reaches an accuracy of G_{thresh} on the validation set, or if it plateaus after T_{plat} iterations. ϕ_M and ϕ_C remain locked in this stage. The detailed algorithm is described in Algorithm 1.

Algorithm 1 Adversarial Gender De-biasing

```

1: Required:  $N_{iter}$ : Number of training iterations
2: Required: Hyperparameters :  $\lambda, K, T_{fc}, G_{thresh}, T_{deb}, T_{gtrain}, T_{plat}, E$ 
3: Required Learning rates:  $\alpha_1, \alpha_2, \alpha_3$ 
4: for  $i$  in 0 to  $N_{iter} - 1$  do
5:   if  $i=0$  then
6:     Perform Stage 1 training update:
7:     for  $p$  in 0 to  $T_{fc} - 1$  do
8:        $\phi_M^{(p)} \leftarrow \phi_M^{(p-1)} - \alpha_1 \nabla_{\phi_M} L_{class}(\phi_M^{(p-1)}, \phi_C^{(p-1)})$ 
9:        $\phi_C^{(p)} \leftarrow \phi_C^{(p-1)} - \alpha_1 \nabla_{\phi_C} L_{class}(\phi_M^{(p-1)}, \phi_C^{(p-1)})$ 
10:    end for
11:   end if
12:   if  $i \bmod E=0$  then
13:     Initialize  $\phi_B$ : Perform Stage 2 training update
14:     for  $q$  in 0 to  $T_{gtrain} - 1$  do
15:        $\phi_B^{(q)} \leftarrow \phi_B^{(q-1)} - \alpha_2 \nabla_{\phi_B} L_g(\phi_M^{(q-1)}, \phi_B^{(q-1)})$ 
16:     end for
17:   end if
18:   Perform Stage 3 training update: ( $\phi_B$  remains locked)
19:   for  $m$  in 0 to  $T_{deb} - 1$  do
20:      $\phi_M^{(m)} \leftarrow \phi_M^{(m-1)} - \alpha_3 \nabla_{\phi_M} L_{br}(\phi_C^{(m-1)}, \phi_M^{(m-1)}, \phi_B^{(m-1)})$ 
21:      $\phi_C^{(m)} \leftarrow \phi_C^{(m-1)} - \alpha_3 \nabla_{\phi_C} L_{br}(\phi_C^{(m-1)}, \phi_M^{(m-1)}, \phi_B^{(m-1)})$ 
22:   end for
23:    $j = i \bmod K$ 
24:   Select gender prediction model  $B_j$ 
25:   for  $n$  in 0 to  $\infty$  do
26:     Compute validation gender prediction accuracy  $A$  of  $B_j$ 
27:     if  $A > G_{thresh}$  or  $n == T_{plat}$  then
28:       break
29:     else
30:       Perform Stage 4 training update: ( $\phi_M, \phi_C$  remain locked)
31:        $\phi_{B_j}^{(n)} \leftarrow \phi_{B_j}^{(n-1)} - \alpha_2 \nabla_{\phi_{B_j}} L_g^{(B_j)}(\phi_M^{(n-1)}, \phi_{B_j}^{(n-1)})$ 
32:     end if
33:   end for
34: end for

```

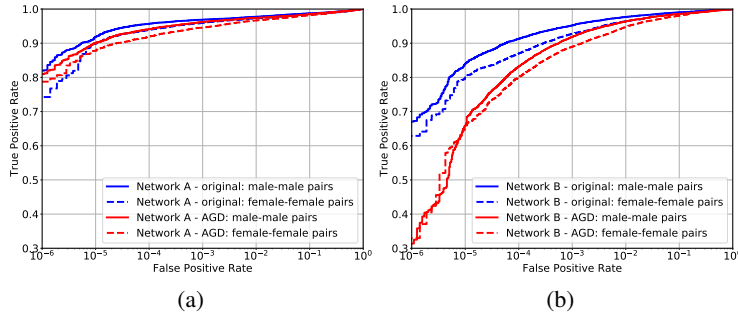


Figure 3: Gender-wise IJB-C verification results for (a.) Network A and (b.) Network B, using features from original pre-trained networks and their AGD counterparts. AGD reduces gender bias at low FPRs.

Table 2: Gender-wise IJB-C verification results and their corresponding gender bias for (a.) Network A and (b.) Network B. AGD has lower bias than CorrPCA at most FPRs. Green: least bias, Yellow: second least bias

FPR	10^{-6}			10^{-5}			10^{-4}			10^{-3}		
Method	TPR _m	TPR _f	Bias									
Original	0.82	0.74	0.08	0.92	0.90	0.02	0.96	0.93	0.03	0.97	0.96	0.01
CorrPCA	0.82	0.76	0.06	0.92	0.90	0.02	0.96	0.93	0.03	0.97	0.96	0.01
AGD	0.81	0.79	0.02	0.90	0.89	0.01	0.94	0.93	0.01	0.96	0.95	0.01

(a) Network A

FPR	10^{-6}			10^{-5}			10^{-4}			10^{-3}		
Method	TPR _m	TPR _f	Bias									
Original	0.67	0.63	0.04	0.84	0.8	0.04	0.92	0.87	0.05	0.96	0.93	0.03
CorrPCA	0.67	0.65	0.02	0.84	0.81	0.03	0.91	0.87	0.04	0.95	0.93	0.02
AGD	0.32	0.32	0.0	0.67	0.67	0.0	0.83	0.81	0.02	0.92	0.90	0.02

(b) Network B

After AGD training, M can generate gender-debiased representation f_{out} for test input feature, which can then be used for face verification. The hyperparameter details and ablation experiments are provided in the supplementary material (Sec. D and E).

6 Results

6.1 AGD versus CorrPCA

CorrPCA results: Referring to Section 5.1, we find that the number of eigenvectors in the subspace G is 8 and 25 for the features of Network A and B respectively. Therefore $|S - G|$ is 504 and 487, for network A and B respectively. Using the transformed feature sets $T_{ijbc}^A \in \mathbb{R}^{n \times 504}$ and $T_{ijbc}^B \in \mathbb{R}^{n \times 487}$, we perform gender-wise IJB-C 1:1 face verification. From Table 2, we can infer that this method helps to reduce the gender bias in Network B, whereas the bias and performance in Network A remains mostly unchanged. We provide the gender-wise verification plots obtained using this method in the supplementary material (Sec. C).

AGD results: After AGD training, we feed the 512 dimensional f_{in} (extracted from either network A or B) of aligned IJB-C images to model M (Fig. 1), which generates 256 dimensional gender de-biased features f_{out} . We then use f_{out} to perform gender-wise IJB-C 1:1 face verification. From Fig. 3. We find that when using f_{out} from network A, the bias is reduced (especially in low FPRs), without catastrophically losing verification performance. This is done by improving female-female verification at low FPRs, while slightly decreasing male-male verification. Similarly, for f_{out} from network B, we find that the gender bias is reduced at low FPRs. The bias is especially close to 0 after FPR 10^{-5} . From Table 2, we can infer that AGD consistently outperforms CorrPCA in terms of bias reduction at almost all the FPRs under consideration. For FPRs not reported in Table 2, the gender bias in verification is exactly same for CorrPCA, AGD and the original pre-trained network. To ensure that CorrPCA and AGD reduce gender information, we perform the following experiment.

Table 3: Accuracy of logistic regression classifier trained using features extracted from original networks, transformed using CorrPCA and extracted using AGD

Method	Network A			Network B		
	Original	CorrPCA	AGD	Original	CorrPCA	AGD
Gender classif ^m acc.	77.09	72.33	64.01	81.02	67.25	75.69

Table 4: IJB-C 1:1 verification results after applying TPE on features of Network B and its AGD counterpart

FPR	10^{-6}			10^{-5}			10^{-4}			10^{-3}		
	Method	TPR _m	TPR _f	Bias	TPR _m	TPR _f	Bias	TPR _m	TPR _f	Bias	TPR _m	TPR _f
Orig. + TPE	0.80	0.69	0.11	0.88	0.84	0.04	0.93	0.89	0.04	0.96	0.94	0.02
AGD + TPE	0.57	0.51	0.06	0.75	0.73	0.02	0.88	0.85	0.03	0.93	0.91	0.02

We train a logistic regression classifier on 60k IJB-C features (30k males and females) to classify gender and test it on 20k IJB-C features (10k males and females). The images for training and testing are selected randomly, and the features are extracted using the pre-trained networks and their de-biased counterparts. From the results in Table 3, we find that for both Networks A and B, the gender classification accuracy goes down when they are extracted using our AGD or CorrPCA framework, which indicates that gender information in the features is likely reduced.

6.2 Analysis of performance drop

Gender is an important face attribute which helps deep networks to recognize faces. So, minimizing its predictability by using AGD is expected to decrease the overall performance as a side-effect. As seen in Fig. 3, the verification performance in Network B reduces considerably as compared to Network A, after AGD is applied. To understand this behavior, we analyze the distribution of the feature space of both networks A and B. For this, we first randomly select 80k images (40k males and females) from the IJB-C dataset, and extract their features using a given pre-trained network (Network A or B). Using PCA, we compute the eigenspace of this feature set. As done in Sec. 5.1, we compute the gender correlation of each of the 512 eigenvectors in the eigenspace (Fig. 4).

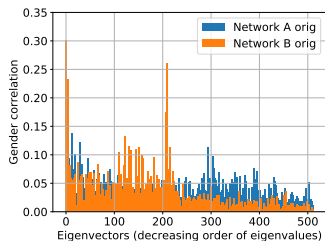


Figure 4: Distribution of gender information in the feature space

In [3], the identity features from Network B are not directly used to perform verification. Instead, the features undergo triplet probabilistic embedding (TPE) [41] for generating a template representation of a given identity. TPE is an embedding learned to generate more discriminative, low-dimensional representations of given input features, that have been shown to achieve better verification results. Using the features of Network B (extracted for UMD-Faces [34] dataset), we learn such an embedding $W_B \in \mathbb{R}^{512 \times 128}$. W_B is then used to transform the IJB-C features extracted using Network B, to obtain 128-dimensional features, which are used for 1:1 face verification. We perform the same experiment with the AGD features of Network B, where a new TPE matrix $W'_B \in \mathbb{R}^{256 \times 128}$ is learned and used to transform the IJB-C AGD features. We find that in both the cases (Network B and its AGD counterpart), *TPE improves the overall verification performance, but it also increases bias at all FPRs*. However, from Table 4, we can infer that the gender bias in the verification results obtained after applying TPE on AGD features is lower than when TPE is applied on original features of Network B. This shows that we can improve the verification performance of AGD features without significantly increasing gender bias. The details of training TPE are provided in the supplementary material (Sec. F).

7 Conclusion and future work

We address the problem of gender bias in face recognition. From our preliminary experiments, we find that balancing the training dataset to include equal number of male and female identities does not necessarily mitigate the issue of gender bias. Motivated by this finding, we aim to reduce gender information in features obtained from the pre-trained networks. We propose two methods for this task. The first method, which acts as a baseline, uses a simple PCA-based technique to remove gender specific components in the feature space. The second method - AGD, adversarially reduces gender information from face recognition features, while training them to classify identities. Both of these methods are agnostic to the gender mix of the training dataset, and the pre-trained networks. We show that AGD significantly outperforms our PCA-based baseline in terms of bias reduction. In the near future, we intend to apply and modify AGD to reduce the information of other attributes like age

and race in face recognition features; and apply a combination of several de-biasing losses to reduce the strength of multiple attributes simultaneously.

Acknowledgement

The authors would like to thank P. Jonathon Phillips, Ankan Bansal and Rajeev Ranjan for their helpful suggestions. This research is based upon work supported by the Office of the Director of National Intelligence (ODNI), Intelligence Advanced Research Projects Activity (IARPA), via IARPA R&D Contract No. 2019-022600002. The views and conclusions contained herein are those of the authors and should not be interpreted as necessarily representing the official policies or endorsements, either expressed or implied, of the ODNI, IARPA, or the U.S. Government. The U.S. Government is authorized to reproduce and distribute reprints for Governmental purposes notwithstanding any copyright annotation thereon.

References

- [1] Schroff, F., D. Kalenichenko, J. Philbin. Facenet: A unified embedding for face recognition and clustering. In *Proceedings of the IEEE Conference on Computer Vision and Pattern Recognition*, pages 815–823. 2015. [1](#)
- [2] Taigman, Y., M. Yang, M. Ranzato, et al. Deepface: Closing the gap to human-level performance in face verification. In *Proceedings of the IEEE Conference on Computer Vision and Pattern Recognition*, pages 1701–1708. 2014.
- [3] Ranjan, R., A. Bansal, J. Zheng, et al. A fast and accurate system for face detection, identification, and verification. *IEEE Transactions on Biometrics, Behavior, and Identity Science*, 1(2):82–96, 2019. [3](#), [8](#)
- [4] Deng, J., J. Guo, X. Niannan, et al. Arcface: Additive angular margin loss for deep face recognition. In *CVPR*. 2019. [1](#), [3](#)
- [5] Bansal, A., R. Ranjan, C. D. Castillo, et al. Deep features for recognizing disguised faces in the wild. In *2018 IEEE/CVF Conference on Computer Vision and Pattern Recognition Workshops (CVPRW)*, pages 10–106. IEEE, 2018. [1](#)
- [6] Grother, P., M. Ngan, K. Hanaoka. Face recognition vendor test (FRVT) part 3: Demographic effects. *National Institute of Standards and Technology*, 2019. [1](#), [2](#)
- [7] Buolamwini, J., T. Gebru. Gender shades: Intersectional accuracy disparities in commercial gender classification. In *Conference on fairness, accountability and transparency*, pages 77–91. 2018. [1](#), [2](#)
- [8] Dhar, P., A. Bansal, C. D. Castillo, et al. How are attributes expressed in face DCNNs? *To appear in 15th IEEE Intl. Conf. Automatic Face and Gesture Recognition*, *arXiv preprint arXiv:1910.05657*, 2020. [1](#), [2](#), [3](#)
- [9] Hill, M. Q., C. J. Parde, C. D. Castillo, et al. Deep convolutional neural networks in the face of caricature: Identity and image revealed. *Nature Mach Intel.* (in press). [2](#), [3](#)
- [10] Parde, C. J., Y. I. Colón, M. Q. Hill, et al. Single unit status in deep convolutional neural network codes for face identification: Sparseness redefined, 2020. [1](#)
- [11] Wang, M., W. Deng, J. Hu, et al. Racial faces in the wild: Reducing racial bias by information maximization adaptation network. In *Proceedings of the IEEE International Conference on Computer Vision*, pages 692–702. 2019. [1](#), [3](#)
- [12] Amini, A., A. P. Soleimany, W. Schwarting, et al. Uncovering and mitigating algorithmic bias through learned latent structure. In *Proceedings of the 2019 AAAI/ACM Conference on AI, Ethics, and Society*, pages 289–295. 2019. [3](#)
- [13] Krishnapriya, K., V. Albiero, K. Vangara, et al. Issues related to face recognition accuracy varying based on race and skin tone. *IEEE Transactions on Technology and Society*, 1(1):8–20, 2020.
- [14] Vangara, K., M. C. King, V. Albiero, et al. Characterizing the variability in face recognition accuracy relative to race. In *Proceedings of the IEEE Conference on Computer Vision and Pattern Recognition Workshops*, pages 0–0. 2019.
- [15] Nagpal, S., M. Singh, R. Singh, et al. Deep learning for face recognition: Pride or prejudiced? *arXiv preprint arXiv:1904.01219*, 2019.
- [16] Furl, N., P. J. Phillips, A. O’Toole. Face recognition algorithms and the other-race effect: Computational mechanisms for a developmental contact hypothesis. *Cognitive Science*, 26:797–815, 2002.
- [17] Cavazos, J. G., P. J. Phillips, C. D. Castillo, et al. Accuracy comparison across face recognition algorithms: Where are we on measuring race bias?, 2019.

- [18] Georgopoulos, M., Y. Panagakis, M. Pantic. Investigating bias in deep face analysis: The kanface dataset and empirical study. *arXiv preprint arXiv:2005.07302*, 2020. 1, 2
- [19] Albiero, V., K. KS, K. Vangara, et al. Analysis of gender inequality in face recognition accuracy. In *Proceedings of the IEEE Winter Conference on Applications of Computer Vision Workshops*, pages 81–89. 2020. 1, 2
- [20] Albiero, V., K. Zhang, K. W. Bowyer. How does gender balance in training data affect face recognition accuracy? *arXiv preprint arXiv:2002.02934*, 2020. 1, 4
- [21] He, K., X. Zhang, S. Ren, et al. Delving deep into rectifiers: Surpassing human-level performance on imagenet classification. In *Proceedings of the IEEE international conference on computer vision*, pages 1026–1034. 2015. 2, 4
- [22] Wang, T., J. Zhao, M. Yatskar, et al. Balanced datasets are not enough: Estimating and mitigating gender bias in deep image representations. In *Proceedings of the IEEE International Conference on Computer Vision*, pages 5310–5319. 2019. 2, 3
- [23] Drozdowski, P., C. Rathgeb, A. Dantcheva, et al. Demographic bias in biometrics: A survey on an emerging challenge. *arXiv preprint arXiv:2003.02488*, 2020. 2
- [24] Gafni, O., L. Wolf, Y. Taigman. Live face de-identification in video. In *Proceedings of the IEEE International Conference on Computer Vision*, pages 9378–9387. 2019. 3
- [25] Wu, Z., Z. Wang, Z. Wang, et al. Towards privacy-preserving visual recognition via adversarial training: A pilot study. In *Proceedings of the European Conference on Computer Vision (ECCV)*, pages 606–624. 2018. 3, 5
- [26] Zhang, B. H., B. Lemoine, M. Mitchell. Mitigating unwanted biases with adversarial learning. In *Proceedings of the 2018 AAAI/ACM Conference on AI, Ethics, and Society*, pages 335–340. 2018. 3
- [27] Madras, D., E. Creager, T. Pitassi, et al. Learning adversarially fair and transferable representations. *arXiv preprint arXiv:1802.06309*, 2018. 3
- [28] Alvi, M., A. Zisserman, C. Nellåker. Turning a blind eye: Explicit removal of biases and variation from deep neural network embeddings. In *Proceedings of the European Conference on Computer Vision (ECCV)*, pages 0–0. 2018. 3
- [29] Li, A., J. Guo, H. Yang, et al. Deepobfuscator: Adversarial training framework for privacy-preserving image classification. *arXiv preprint arXiv:1909.04126*, 2019. 3
- [30] Choi, J., C. Gao, J. C. Messou, et al. Why Can’t I Dance in the Mall? Learning to Mitigate Scene Bias in Action Recognition. In *Advances in Neural Information Processing Systems*, pages 851–863. 2019. 3
- [31] Quadrianto, N., V. Sharmanska, O. Thomas. Discovering fair representations in the data domain. In *Proceedings of the IEEE Conference on Computer Vision and Pattern Recognition*, pages 8227–8236. 2019. 3
- [32] Sattigeri, P., S. C. Hoffman, V. Chenthamarakshan, et al. Fairness GAN. *arXiv preprint arXiv:1805.09910*, 2018. 3
- [33] Liu, Z., P. Luo, X. Wang, et al. Deep learning face attributes in the wild. In *Proceedings of International Conference on Computer Vision (ICCV)*. 2015. 3
- [34] Bansal, A., A. Nanduri, C. D. Castillo, et al. Umdfaces: An annotated face dataset for training deep networks. In *2017 IEEE International Joint Conference on Biometrics (IJCB)*, pages 464–473. IEEE, 2017. 3, 4, 5, 8, 12
- [35] Bansal, A., C. D. Castillo, R. Ranjan, et al. The do’s and don’ts for CNN-based face verification. In *Proceedings of the IEEE International Conference on Computer Vision*, pages 2545–2554. 2017. 3, 4, 5, 12
- [36] Guo, Y., L. Zhang, Y. Hu, et al. Ms-celeb-1m: A dataset and benchmark for large-scale face recognition. In *European Conference on Computer Vision*, pages 87–102. Springer, 2016. 3, 4, 5, 12
- [37] Maze, B., J. Adams, J. A. Duncan, et al. IARPA janus benchmark-c: Face dataset and protocol. In *2018 International Conference on Biometrics (ICB)*, pages 158–165. IEEE, 2018. 3, 4, 5, 13
- [38] Klambauer, G., T. Unterthiner, A. Mayr, et al. Self-normalizing neural networks. In *Advances in neural information processing systems*, pages 971–980. 2017. 5
- [39] Ranjan, R., S. Sankaranarayanan, C. D. Castillo, et al. An all-in-one convolutional neural network for face analysis. In *2017 12th IEEE International Conference on Automatic Face & Gesture Recognition (FG 2017)*, pages 17–24. IEEE, 2017. 5
- [40] Turk, M., A. Pentland. Face recognition using eigenfaces. In *Proceedings. 1991 IEEE computer society conference on computer vision and pattern recognition*, pages 586–587. 1991. 5

- [41] Sankaranarayanan, S., A. Alavi, C. D. Castillo, et al. Triplet probabilistic embedding for face verification and clustering. In *2016 IEEE 8th International Conference on Biometrics Theory, Applications and Systems (BTAS)*. 2016. 8, 15

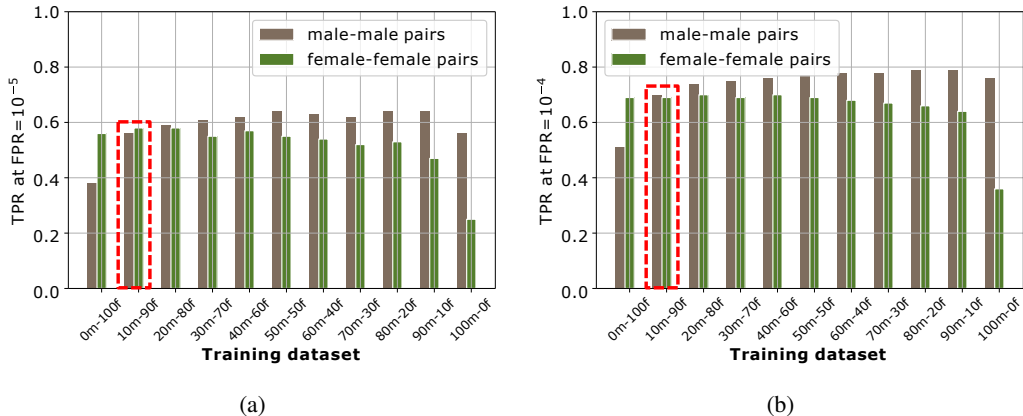


Figure 5: Gender-wise IJB-C face verification results at (a.) $FPR=10^{-5}$ and (b.) $FPR=10^{-4}$, after training on datasets with different gender-mix. We find that the network trained on $10m-90f$ dataset achieves lowest bias at both of these FPRs. However, finding such an appropriate gender-mix is not scalable.

A Effect of gender-mix in training datasets on gender bias

As mentioned in Section 3.2 of the main paper, we built 11 alternative training datasets using subsets of UMDFaces [34], UMDFaces-Videos [35] and MS-Celeb-1M [36] datasets. Each of these alternative datasets consists of 14,815 identities and a different gender mix (i.e. a different ratio of male and female identities). Every identity consists of exactly 50 images. We name the dataset as ‘ $Xm-Yf$ ’ where X, Y denote the percentage of male and female identities in the dataset, respectively. For example, $30m-70f$ represents an alternative dataset with 30% male and 70% female identities. Using these datasets, we train a network with the same architecture and loss function as that of Network B. Using the final fully connected layer of the trained network, we extract the features for aligned IJB-C faces and perform gender-wise 1:1 face verification. In the main paper, we show that the network trained on $50m-50f$ dataset does not have minimum gender bias. Instead the network achieves a gender-balanced performance when the training dataset is $10m-90f$ (i.e. it consists of 90% female and 10% male identities). Here, in Fig. 5, we present the verification results of male-male female-female pairs for all the 11 alternative training datasets, at $FPR=10^{-5}$ and $FPR=10^{-4}$. We also observe that for all the alternative datasets consisting of less than 90% female identities, the gender-bias (i.e. the difference between male and female TPR) increases as we decrease the percentage of female identities.

B Baseline (CorrPCA) algorithm

In Sec. 5.1 of the main paper, we introduce a baseline method: Correlation-based PCA (CorrPCA) to isolate and remove gender specific components in the feature space. Here, we provide the detailed algorithm for the same in Algorithm 2. X denotes the set of 512 dimensional features extracted for images in the training set, using Network A or B. G indicates the set of eigenvectors which have high correlation with gender. $S - G$ represents the set of eigenvectors in S which are not in G . In our experiments, we use Spearman correlation to compute coefficient κ . Also, we use $\delta = 0.1$, to select the gender-encoding eigenvectors.

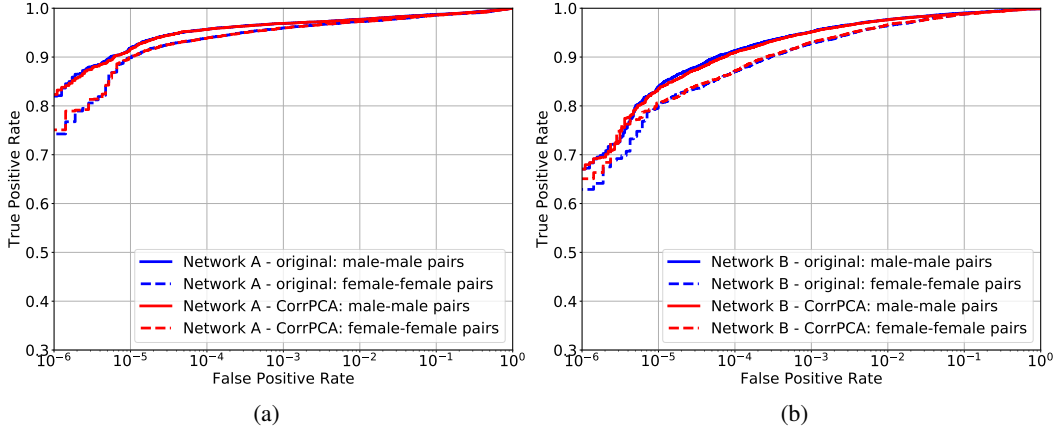


Figure 6: Gender-wise IJB-C face verification results (a.) Network A and (b.) Network B, using features transformed with CorrPCA

Algorithm 2 CorrPCA

- 1: **Required:** Training feature set : X
 - 2: **Required:** Gender labels for training feature set : ℓ
 - 3: **Required:** Hyperparameter : δ
 - 4: Compute Eigenspace $S = PCA(X)$
 - 5: Gender specific eigenvector set $G = []$
 - 6: **for** s in S **do**
 - 7: $v_s = X \cdot s$
 - 8: Compute correlation coefficient $\kappa = Corr(v_s, \ell)$
 - 9: **if** $\kappa > \delta$ **then**
 - 10: $G \leftarrow s$
 - 11: **end if**
 - 12: **end for**
 - 13: Return $G, S - G$
-

After this, we use the set $S - G$ to transform test features from IJB-C dataset [37], and use them for 1:1 face verification.

C Gender-wise verification plots - CorrPCA

We present the gender-wise verification plots on the IJB-C dataset obtained after using the face recognition features transformed using the CorrPCA baseline. We also include the results using the original features from pre-trained networks (Network A or B). From Fig. 6b, we find that CorrPCA helps to reduce the gender bias in Network B, especially between FPR 10^{-5} and 10^{-6} . However, as seen in Fig. 6a, the bias and performance in Network A remains mostly unchanged. The gender-wise TPRs and bias values are provided in Table 2 in the main paper.

D Hyperparameter information for AGD

We explained the training scheme of Adversarial Gender De-biasing (AGD) in Section 5.2 in the main paper. Here, we specify the hyperparameters used in different stages.

Stage 1 : We train M and C for $T_{fc} = 66000$ iterations with a learning rate $\alpha_1 = 10^{-5}$. L_{class} is used for optimizing the weights of M and C .

Stage 2 : We train the gender prediction models (GPMs), using L_g , for $T_{gtrain} = 30000$ iterations with a learning rate $\alpha_2 = 10^{-3}$. Here, we use $K = 1$ and 5 for Network A and B, respectively.

Stage 3 : In this stage, we train model M and classifier C using L_{br} , for $T_{deb} = 1200$ iterations, with a learning rate of $\alpha_3 = 10^{-4}$. We compute L_{br} using $\lambda = 10$ and 1 , when using f_{in} from Networks A and B respectively.

Stage 4 : We re-train the heuristically chosen GPM (with a learning rate of α_2 , as done in stage

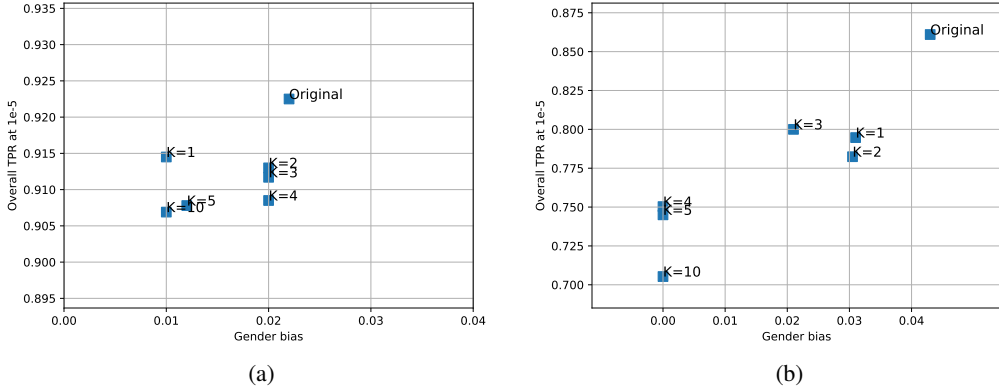


Figure 7: TPR (at $FPR=10^{-5}$) versus Bias for different K used to train AGD frameworks on (a.) Network A (b.) Network B

2) until it achieves an accuracy of G_{thresh} or until it plateaus after $T_{plat} = 2000$ iterations. We use $G_{thresh} = 0.90$ and 0.80 for networks A and B, respectively. After a fixed number of episodes ($E = 30$) of running stage 3 and 4, we re-initialize all the GPMs and re-train them, as done in Stage 2.

In all the aforementioned training stages, we use an Adam optimizer and a batch size of 400, and we ensure that each batch is balanced in terms of gender.

E Ablation study - AGD

In the main paper, we define the loss used for training Adversarial Gender De-biasing (AGD) framework as follows:

$$L_{br}(\phi_C, \phi_M, \phi_B) = L_{class}(\phi_C, \phi_M) + \lambda L_{deb}(\phi_M, \phi_B) \quad (9)$$

Here, we evaluate two hyperparameters used for training the AGD framework : (a.) the number of gender prediction models (GPMs) K in the ensemble used to compute L_{deb} . This is also defined in Section 4.1 in the main paper and, (b.) the weight for L_{deb} defined in Eq. 9. We analyze how changing these hyperparameters vary the resultant bias reduction and verification performance at a fixed $FPR = 10^{-5}$.

We first vary the number of GPMs K and experiment with $K = 1, 2, 3, 4, 5$ and 10 . Here, other than K , we fix all the other hyperparameters and use the same values specified in the previous section. In Fig. 7, we find that in network A, changing K does not have much effect on gender bias or verification TPR at $FPR 10^{-5}$. However, for network B, we find that as we increase K , the gender bias keeps decreasing which in turn leads to drop in verification performance at $FPR 10^{-5}$. We find that at $K = 4$, the bias drops to 0, and as we further keep increasing K , the verification performance decreases.

After this, we perform experiments to observe the effect of parameter λ which is used to weight L_{deb} in Eq. 9. We fix $K = 5$ and evaluate $\lambda = 0.1, 1, 10$ for training the AGD framework using f_{in} from Network A and B (using the values in previous section for other hyperparameters). The results are presented in Fig. 8. We find that for Network A, as we keep on increasing the value of λ , the gender bias keeps generally decreasing and the verification TPR keeps decreasing. For Network B, we can draw a similar conclusion. However using $\lambda = 0.1$ and 1 , we obtain a similar verification TPR, although the bias when using $\lambda = 0.1$ is considerably higher.

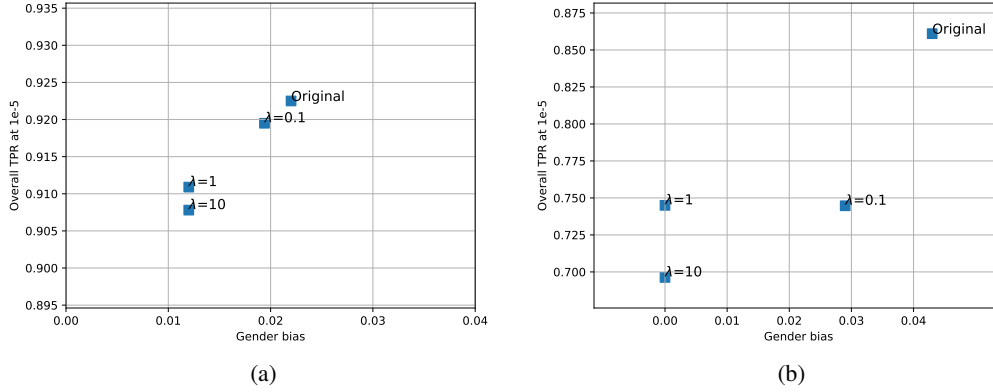


Figure 8: TPR (at $FPR=10^{-5}$) versus Bias for different λ used to train AGD frameworks on (a.) Network A (b.) Network B

F Training details for Triplet Probabilistic Embedding

For training a TPE matrix, we use a fixed learning rate of 2.5×10^{-3} and a batch size of 32. The training for computing such a matrix using the features from Network B (or its AGD counterpart) generally converges after 10k iterations. For a given set of features, we compute its TPE matrix ten times and finally compute the average of the resulting matrices. We use this matrix to transform the test features. More details about TPE are provided in [41].